

Numerical evidence for the non-Abelian eigenstate thermalization hypothesis and a non-Abelian fluctuation-dissipation theorem

Jade LeSchack,¹ Aleksander Lasek,¹ Jae Dong Noh,² and Nicole Yunger Halpern^{1,3}

¹*Joint Center for Quantum Information and Computer Science,
NIST and University of Maryland, College Park, Maryland 20742, USA*

²*Department of Physics, University of Seoul, Seoul 02504, Korea*

³*Institute for Physical Science and Technology, University of Maryland, College Park, MD 20742, USA*

(Dated: June 4, 2025)

Noncommutation is fundamental to quantum theory. The incompatibility of observables is one crucial difference between classical and quantum mechanics. Thermodynamic laws must apply across classical and quantum systems. Historically, researchers have implicitly assumed that conserved quantities in thermodynamic systems commute with each other. When we remove this assumption, conserved quantities that fail to commute with each other in thermodynamics engender new physics. One seminal result in thermodynamics for closed quantum many-body systems is the eigenstate thermalization hypothesis (ETH), which explains how a quantum many-body system thermalizes internally. The ETH applies across many fields including atomic, molecular, and optical physics, condensed-matter physics, and high-energy physics. Murthy *et al.* recently showed that the ETH does not apply to systems with noncommuting conserved quantities. Murthy *et al.* posited a non-Abelian ETH to account for systems with noncommuting conserved quantities. We calculate numerics to support the non-Abelian ETH. We model a one-dimensional (1D) next-nearest-neighbor Heisenberg chain of 18 qubits. We represent local operators with matrices relative to an energy eigenbasis. Our numerics evidence the non-Abelian ETH's qualitative predictions. Noh *et al.* also recently derived a fluctuation-dissipation theorem (FDT) from the ETH. With the recently proposed non-Abelian ETH, we begin numerical calculations in support of an FDT derived from the non-Abelian ETH. We offer the first comprehensive numerical tests of the non-Abelian ETH and initial numerics for deriving an FDT for systems that follow the NAETH.

I. INTRODUCTION

We expect thermodynamic laws to hold no matter the regime – classical or quantum, relativistic or non-relativistic. Thermodynamics was born from the industrial revolution as scientists and engineers asked questions about energy, work, and efficiency. Scientists could describe macroscopic properties and processes such as temperature and energy transformation without worrying about the microscopic interactions of matter. Consider the second law of thermodynamics; it states that the entropy of a system must remain constant or increase. A consequence of this law is that systems in thermal contact with each other tend to thermalize. This is typically true for both macroscopic objects and quantum-mechanical particles. In the rapidly growing field of quantum thermodynamics, researchers apply tools from quantum information to thermodynamic laws for both fundamental understanding and practical applications [1, 2].

An active area of quantum thermodynamics is the subfield of noncommuting charges (conserved quantities) [3]. Consider a system S that exchanges globally conserved quantities Q_a^{tot} and Q_b^{tot} with an environment E . Figure 1 illustrates the setup. Historically, in both classical and quantum thermodynamics, researchers implicitly assumed that $[Q_a^{\text{tot}}, Q_b^{\text{tot}}] = 0$ [4–6]. The subfield of noncommuting charges focuses on systems where we remove this assumption, i.e., $[Q_a^{\text{tot}}, Q_b^{\text{tot}}] \neq 0$. The Hamiltonians of such systems have a non-Abelian symmetry, so this subfield is also called non-Abelian quantum thermody-

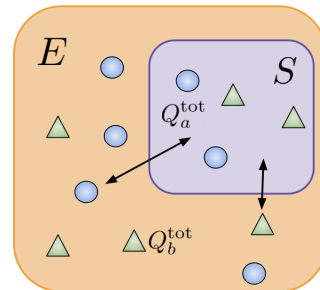


FIG. 1: A system S exchanging quantities Q_a^{tot} and Q_b^{tot} with an environment E . The quantities are globally conserved, so we also call them charges. Figure adapted from [3]

namics. Noncommuting charges give rise to changes in thermodynamic phenomena. Changed thermodynamic phenomena include thermodynamic-entropy production [7, 8] and many-body localization [9, 10]. Noncommutation is a cornerstone of quantum theory, and understanding how noncommutation affects thermodynamic phenomena is foundational to thermal physics.

One thermodynamic phenomenon that noncommutation of charges impacts is thermalization in closed quantum systems. A closed quantum system challenges the second law of thermodynamics because the system evolves unitarily such that its von Neumann entropy remains constant. The second law of thermodynamics says

that thermalization increases a system's entropy. Therefore, we do not expect a closed quantum system to thermalize. However, such systems thermalize internally in the sense that local operators' expectation values over time approximately equal their thermal expectation values. The eigenstate thermalization hypothesis (ETH) governs this internal thermalization for systems with non-degenerate, non-integrable Hamiltonians [11–13]. The ETH has applications to atomic, optical, and molecular (AMO) physics, quantum chaos, condensed-matter physics, and high-energy physics [14, 15]. A system with a non-Abelian symmetry as shown in Fig. 1 does not follow the ETH [16]. Murthy *et al.* posited the non-Abelian ETH (NAETH) for Hamiltonians with non-Abelian symmetries [16]. Noh began numerical studies of the NAETH [17]. He studied local operators on a two-dimensional XXZ Heisenberg model both with and without an SU(2) symmetry. He found that the matrix elements of local operators represented in the Hamiltonian energy basis follow the ETH in both cases. When the model had an SU(2) symmetry (a non-Abelian symmetry), the matrix elements also followed a prediction of the NAETH for certain eigenspaces. The SU(2)-symmetric model had additional symmetries aside from the SU(2) symmetry. My work continues these studies with Lasek, Noh, and Yunger Halpern to provide the first comprehensive numerical support for the NAETH's predictions [18]. We numerically evidence the NAETH for a model with only SU(2) symmetry and no extraneous symmetries.

Systems tend to thermalize to a thermal state, which is a stationary state. The fluctuation-dissipation theorem (FDT) describes how a system in a stationary state responds to small perturbations and relates the dynamic response function and time correlation function [19, 20]. The quantum-mechanical FDT is derived from the Gibbs state, a thermal stationary state. Noh *et al.* showed that a FDT can be derived from the ETH for generic quantum many-body systems, not just the stationary Gibbs state [21]. We seek to extend this work to quantum many-body systems with a non-Abelian symmetry as we may be able to derive an FDT for such systems from the NAETH. We calculate numerical statistics to support the NAETH's predictions and to derive an FDT from the NAETH. This thesis draws from work completed in [18] and a pre-print in preparation [22].

Our numerics confirm four qualitative predictions of the NAETH and support preliminary work for a FDT for closed quantum-many body systems with a non-Abelian symmetry. First, we verify that our Heisenberg model's Hamiltonian is suitable for testing the NAETH. We check statistics from random-matrix theory and find that our Hamiltonian is non-integrable, a requirement for a system to follow the NAETH. Then, we investigate the block-diagonal and off-block-diagonal terms in the NAETH for a subsector. In our last test of the NAETH, we plot functions in the NAETH equation and confirm that they are smooth. We detail one method for obtaining those smooth functions. We use those smooth func-

tions in a preliminary statistic for the FDT. Significance - contribute to the first thorough numerical support of the NAETH.

The rest of this thesis is organized as follows. In Sec. II, we review technical background on the ETH, the NAETH, the FDT, and the KMS condition. Next, in Sec. III, we discuss the methods of our numerical analysis. Following that, in Sec. IV, we present our results from testing the NAETH and initial checks of a non-Abelian FDT. In Sec. V, we draw our conclusions and discuss future outlook from the work.

II. TECHNICAL INTRODUCTION

This section reviews relevant background information. In Sec. II A, we review the ETH and which conditions a system must satisfy for the ETH to apply. In Sec. II B, we introduce spherical tensor operators, which we will use to analyze the NAETH. There we also introduce the NAETH and the kinds of systems that the NAETH governs. Lastly, in Sec. II C, we review the FDT, the Kubo-Martin-Schwinger (KMS) condition, and their connection to the ETH.

II A. ETH

Consider a closed quantum many-body system governed by a nonintegrable Hamiltonian H that lacks non-Abelian symmetries. H has eigenvalues E_α associated with eigenstates $|\alpha\rangle$. Let A be a local operator and H be a non-integrable many-body Hamiltonian. A can be represented as a matrix relative to the energy eigenbasis. The ETH is an ansatz for the forms of those matrix elements $\langle\alpha|A|\alpha'\rangle$. For a matrix element $\langle\alpha|A|\alpha'\rangle$, let $\mathcal{E} := (E_\alpha + E_{\alpha'})/2$ be the average energy between E_α and $E_{\alpha'}$. Let $\omega := (E_\alpha - E_{\alpha'})$ be the difference in energies. $\mathcal{A}(\mathcal{E})$ is a smooth, real function denoting the microcanonical average of A . $f(\mathcal{E}, \omega)$ is also a smooth, real function. The thermodynamic entropy $S_{\text{th}}(\mathcal{E})$ is the natural logarithm of the density of states. R is a matrix with random values. A and H satisfy the ETH if

$$\langle\alpha|A|\alpha'\rangle = \mathcal{A}(\mathcal{E}) \delta_{\alpha\alpha'} + e^{-S_{\text{th}}(\mathcal{E})/2} f(\mathcal{E}, \omega) R_{\alpha\alpha'}. \quad (1)$$

We call the first term $\mathcal{A}(\mathcal{E}) \delta_{\alpha\alpha'}$ the diagonal term; it is nonzero only for matrix elements along the diagonal. We dub the ETH's second term $e^{-S_{\text{th}}(\mathcal{E})/2} f(\mathcal{E}, \omega) R_{\alpha\alpha'}$ the off-diagonal term.

II B. Spherical tensor operators and NAETH

For a Hamiltonian with a non-Abelian symmetry, spherical tensor operators are convenient local operators for computing expectation values and matrix elements. To introduce spherical tensor operators, we introduce

the setup that applies throughout the rest of the thesis. Consider a quantum many-body system with an SU(2)-symmetric Hamiltonian H and $N \gg 1$ quantum bits (qubits). The global spin components are $S_{a=x,y,z}$ and the global spin-squared operator is \vec{S}^2 . H shares an eigenbasis $\{|\alpha, m\rangle\}$ with \vec{S}^2 and S_z . The eigenenergies E_α and total spin quantum numbers s_α are labelled by α . m is the total spin magnetic quantum number. Throughout the paper, we set $\hbar = 1$. We have the following relations:

$$H|\alpha, m\rangle = E_\alpha|\alpha, m\rangle, \quad (2)$$

$$\vec{S}^2|\alpha, m\rangle = s_\alpha(s_\alpha + 1)|\alpha, m\rangle, \quad \text{and} \quad (3)$$

$$S_z|\alpha, m\rangle = m|\alpha, m\rangle. \quad (4)$$

The commutation relations

$$[S_z, T_q^{(k)}] = \hbar q T_q^{(k)} \quad \text{and} \quad (5)$$

$$[S_\pm, T_q^{(k)}] = \hbar \sqrt{(k \mp q)(k \pm q + 1)} T_{q\pm 1}^{(k)} \quad (6)$$

fully define the spherical tensor operators $T_q^{(k)}$ [23]. The raising and lowering operators are $S_\pm := S_x \pm iS_y$. The rank k resembles s_α , and $q = -k, -k + 1, \dots, k$ resembles m . Spherical tensor operators transform irreducibly under SU(2).

The Wigner-Eckart theorem is a fundamental theorem in quantum mechanics that stipulates the form of a spherical tensor operator's matrix elements [23]. Such matrix elements are the product of two factors: a Clebsch-Gordon coefficient and a reduced matrix element $\langle \alpha || T^{(k)} || \alpha' \rangle$. (A reduced matrix element is a matrix element divided out by a Clebsch-Gordon coefficient.) Non-Abelian symmetries invalidate the ETH because the matrix-element forms stipulated by the Wigner-Eckart theorem do not necessarily match the ETH's predictions [16].

Now, we introduce the NAETH. As in Sec. II A, the average energy is $\mathcal{E} := (E_\alpha + E_{\alpha'})/2$, and the difference in energies is $\omega := (E_\alpha - E_{\alpha'})$. We also define the average spin quantum number $\mathcal{S} := (s_\alpha + s_{\alpha'})/2$ and the difference in spin quantum numbers $\nu := (s_\alpha - s_{\alpha'})$. $S_{\text{th}}(\mathcal{E}, \mathcal{S})$ remains the thermodynamic entropy. The NAETH is an ansatz for the forms of reduced matrix elements $\langle \alpha || T^{(k)} || \alpha' \rangle$ of a spherical tensor operator $T_q^{(k)}$. Let $\mathcal{T}^{(k)}(\mathcal{E}, \mathcal{S})$ be an $O(1)$ smooth function that depends on the rank k of the spherical tensor operator, \mathcal{E} , and \mathcal{S} . Let $f_\nu^{(T)}(\mathcal{E}, \mathcal{S}, \omega)$ be an $O(1)$ smooth function that depends on the spherical tensor operator T , ν , \mathcal{E} , and \mathcal{S} . $R_{\alpha\alpha'}^{(T)}$ is a matrix with values that follow a normal distribution. The NAETH says that [16]

$$\langle \alpha || T^{(k)} || \alpha' \rangle = \mathcal{T}^{(k)}(\mathcal{E}, \mathcal{S}) \delta_{\alpha\alpha'} + e^{-S_{\text{th}}(\mathcal{E}, \mathcal{S})/2} f_\nu^{(T)}(\mathcal{E}, \mathcal{S}, \omega) R_{\alpha\alpha'}^{(T)}. \quad (7)$$

This assumption about the reduced matrix elements' forms, together with additional assumptions, implies thermalization of a closed quantum many-body system with a non-Abelian symmetry in some cases.

II C. The FDT and the KMS condition

The FDT describes how quickly a system responds to small perturbations [19, 20]. Consider a quantum system with a Hamiltonian H in an initial state ρ_i at time t_i . For an observable B , a time-dependent perturbation $\delta H = -\hbar(t)B$ applied to the system causes the expectation value of an observable A at some time $t' > t_i$ to deviate from its unperturbed value. Define the correlation function $\bar{S}_{AB}(t, t') := \langle A(t)B(t') \rangle_i - \langle A(t) \rangle_i \langle B(t') \rangle_i$, which depends on the expectation value $\langle \cdot \rangle_i$ of the state ρ_i . The deviation δA depends on the linear-response function

$$\chi''_{AB}(t, t') := \frac{1}{2\hbar} (\bar{S}_{AB}(t, t') - \bar{S}_{BA}(t', t)). \quad (8)$$

The correlation functions obey the KMS condition

$$\bar{S}_{AB}(t) = \bar{S}_{BA}(-t - i\beta\hbar). \quad (9)$$

The FDT dictates the relationship between the linear-response function and the correlation function. From linear-response theory and the KMS condition, the fluctuation-dissipation theorem is

$$\chi''_{AB, \text{eq}}(\omega) = \frac{1 - e^{-\beta\hbar\omega}}{2\hbar} \bar{S}_{AB, \text{eq}}(\omega). \quad (10)$$

Noh *et al.* derived expressions for correlation functions $\bar{S}_{AB}(\omega)$ found in the FDT from the ETH [21]. They apply the ETH to the operators A and B in $\bar{S}_{AB}(\omega)$. A finite-system-size correction term appears in their analytic derivation. The correction term disappears in the limit of infinite system size. We extend Noh's work to quantum many-body systems with a non-Abelian symmetry. Such systems might satisfy the NAETH. We ask: Do systems that follow the NAETH also satisfy the KMS condition? Our numerics in progress work toward answering that question. We have analytically calculated the finite-system-size correction to an FDT derived from the NAETH. The expression for the correction term is

$$\ln \left[\frac{\bar{S}_{AA}(\omega)}{\bar{S}_{AA}(-\omega)} \right] - \beta\omega \simeq \frac{\sum_{\nu=-k}^k \nu X(\nu|k) \mathcal{F}_{AA}(E_\alpha, s_\alpha; \omega; \nu)}{\sum_{\nu} X_e(\nu) \mathcal{F}_\nu(E_0, s_0, \omega)} + \frac{\sum_{\nu} \nu X_e(\nu) \frac{\partial \mathcal{F}_\nu}{\partial \mathcal{S}}(E_0, s_0, \omega)}{\sum_{\nu} X_e(\nu) \mathcal{F}_\nu(E_0, s_0, \omega)}. \quad (11)$$

We will use this equation to begin numerical calculations that aid in deriving an FDT from a system that follows the NAETH.

III. METHODS

In this section, we review the particular SU(2)-symmetric Hamiltonian that we numerically model to test the NAETH's predictions. The physical system that we model is a 1D chain of $N = 18$ qubits with open

boundary conditions. Let $\sigma_a^{(j)}$ be the a -component of spin for the j -th site for $a \in \{x, y, z\}$. The Hamiltonian of the system is

$$H = \sum_{j=1}^{N-1} J_j \vec{\sigma}^{(j)} \cdot \vec{\sigma}^{(j+1)} + \sum_{j=1}^{N-2} \frac{J}{2} \vec{\sigma}^{(j)} \cdot \vec{\sigma}^{(j+2)}. \quad (12)$$

The Hamiltonian is non-integrable due to next-nearest-neighbor couplings. This model globally conserves total spin components defined by $\sigma_a^{\text{tot}} := \sum_{j=1}^N \sigma_a^{(j)}$, i.e. $[H, \sigma_a^{\text{tot}}] = 0 \forall a = x, y, z$. However, the total spin components do not commute with each other: $[\sigma_a^{\text{tot}}, \sigma_b^{\text{tot}}] \neq 0$ if $a \neq b$.

We eigensolve the Hamiltonian exactly via two computational procedures. Our choice of procedure depends on the system size. For $N \geq 16$ qubits, we use the Intel Math Kernel Library and parallel-computing clusters with large-sparse-matrix operations. For smaller system sizes ($N \leq 14$), we use the Quantum Toolbox in Python (QuTiP) package. We build the spherical tensor operators in Python and store the matrix elements $\langle \alpha || T_q^{(k)} || \alpha \rangle$.

IV. RESULTS AND DISCUSSION

In this section, we describe our findings from our tests of the NAETH. In Sec. IV A, we showcase four calculations that evidence the NAETH's qualitative predictions. We analyze the block-diagonal and off-block-diagonal reduced matrix elements of a $T_0^{(1)}$ operator. We also plot $f_\nu^{(T)}(\mathcal{E}, \mathcal{S}, \omega)$ functions and check if they are smooth. In Sec. IV B, we discuss the in-progress work to determine whether the NAETH satisfies the KMS condition. These numerics require $f_\nu^{(T)}(\mathcal{E}, \mathcal{S}, \omega)$ functions. We discuss each result's significance after displaying it.

IV A. Support for the NAETH

In this subsection, we review four qualitative predictions of the NAETH and ancillary calculations supporting the main numerics. As a prelude to the primary results, we confirm that the Hamiltonian is nonintegrable by plotting energy-gap statistics.

The first statistic we plot is the probability-density function of the minimal energy-gap ratio between consecutive eigenenergies. This statistic confirms that H is nonintegrable and so should obey the NAETH [24]. For a given eigenenergy E_n , consider $E_{n+1} - E_n$ and $E_n - E_{n-1}$, which are the differences between E_n and its neighboring energy levels. The minimal gap ratio is

$$R_n := \min \left\{ \frac{E_{n+1} - E_n}{E_n - E_{n-1}}, \frac{E_n - E_{n-1}}{E_{n+1} - E_n} \right\}. \quad (13)$$

We compute the probability density distribution that any given gap ratio is of size r . We fit the prediction cal-

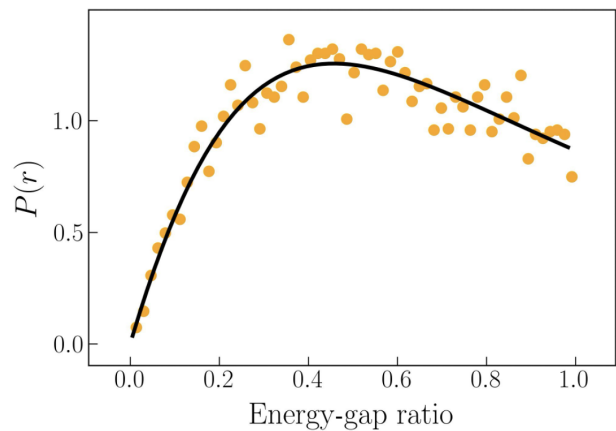


FIG. 2: Scatter plot displaying the probability density of minimal gap ratio values for a system of 18 qubits' $s_\alpha = 3$, $m = 0$ eigenspace. The black curve is the equation $P_{\text{GOE}}(r)$ from random-matrix theory of Gaussian orthogonal ensembles. The black curve fits the data points well with $R^2 = 0.883$, suggesting that the Hamiltonian is nonintegrable.

culated from the random-matrix theory of Gaussian orthogonal ensembles, $P_{\text{GOE}}(r) = \frac{27}{4} \frac{r(1+r)}{(1+r+r^2)^{5/2}}$ [24] to the computed distribution. Figure 2 shows an example of the gap-ratio plot and fitted prediction curve for 18 qubits in the $s_\alpha = 3$, $m = 0$ eigenspace. The linear-regression coefficient for the black curve fitted to the data points is $R^2 = 0.883$, which suggests that curve fits the data well. This fit is evidence for the Hamiltonian's nonintegrability.

In our first test of the NAETH, we plot the reduced matrix elements of a $T_0^{(1)}$ operator in Fig. 3. The elements form bands distinguished by s_α values. The reduced matrix elements in each band vary in a manner that suggests smoothness. Within each band, the elements have a finite variance around a mean value, behavior typical of a distribution governed by a smooth function rather than randomness. The smoothness of the distribution is consistent with the $\mathcal{T}^k(\mathcal{E}, \mathcal{S})$ in the NAETH.

Next, we test the NAETH's second term (see Eq. 7). We subtract the smooth functions evidenced in Fig. 3 from $\langle \alpha || T^{(1)} || \alpha \rangle$ by fitting a linear function to each s_α band and subtracting it from that band's matrix elements. This subtraction should leave us with elements that follow a Gaussian distribution due to the $R_{\alpha\alpha'}^{(T)}$ in the NAETH's second term. Figure 4 displays the resulting plot after we shift the block-diagonal reduced matrix elements to remove the mean element. A Gaussian distribution fits to the data well as the black line in Fig. 4 shows. These numerics support the NAETH's prediction of the second term's form.

Third, we continue to test the NAETH's second term, but now we consider the off-block-diagonal reduced matrix elements. Because of the kronecker delta $\delta_{\alpha\alpha'}$ in the first term of the NAETH (Eq. 7), the first term

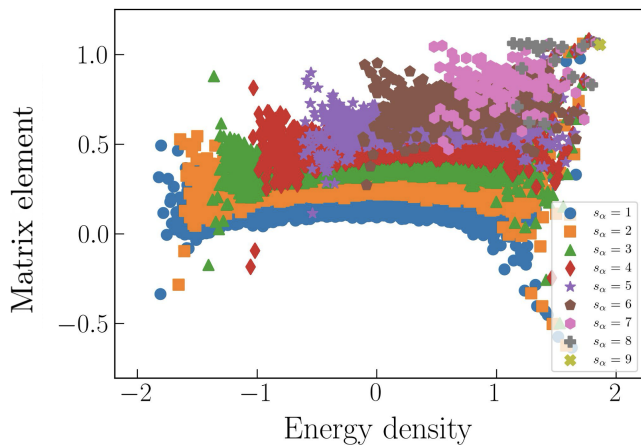


FIG. 3: Reduced matrix elements $\langle \alpha || T^{(1)} || \alpha \rangle$ versus energy density E_α/N for different s_α sectors.

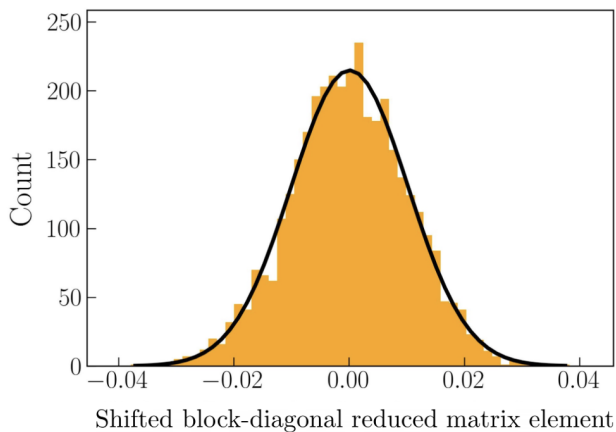


FIG. 4: Histogram of block-diagonal reduced matrix elements $\langle \alpha || T^{(1)} || \alpha \rangle$ for $s_\alpha = 3$. The elements are shifted as we subtract the mean element from the reduced-matrix-element values. A normal distribution (shown by the black curve) fits the histogram, which we expect from $R_{\alpha\alpha}^{(T)}$ in the NAETH's second term.

vanishes for off-block-diagonal reduced matrix elements $\langle \alpha || T^{(1)} || \alpha' \rangle$ when $\alpha \neq \alpha'$. Therefore, we plot a histogram of the off-block-diagonal reduced matrix elements $\langle \alpha || T^{(1)} || \alpha' \rangle$ for $s_\alpha = 3$ in Fig. 5. We expect that the elements follow a Gaussian distribution due to the $R_{\alpha\alpha'}^{(T)}$ in the NAETH's second term. Our numerics support that expectation as evidenced by the black curve's close fit to the histogram in Fig. 5; the black curve is a Gaussian distribution.

Lastly, we qualitatively test the $f_\nu^{(T)}(\mathcal{E}, \mathcal{S}, \omega)$ functions that appear in the second term of the NAETH (Eq. 7). We plot $|f_\nu^{(T)}(\mathcal{E} = 0, \omega)|$ for different values of \mathcal{S} and ν in Fig. 6. The NAETH says the functions should be smooth. Despite our finite-system-size numerics yielding discrete s_α and E_α values, the plots suggest

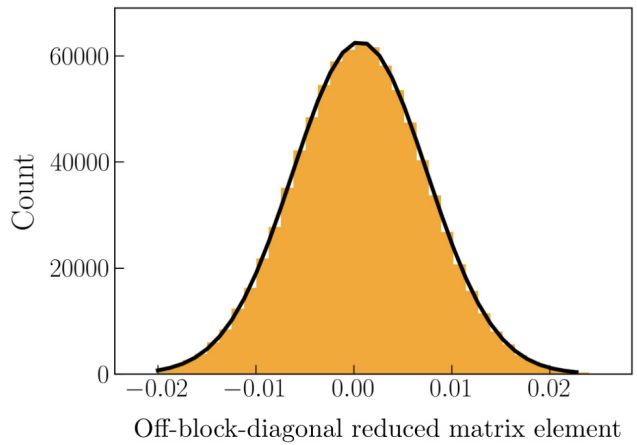


FIG. 5: Histogram of off-block-diagonal reduced matrix elements $\langle \alpha || T^{(1)} || \alpha' \rangle$ for $s_\alpha = 3$. A normal distribution (shown by the black curve) fits the histogram, which we expect from $R_{\alpha\alpha'}^{(T)}$ in the NAETH's second term.

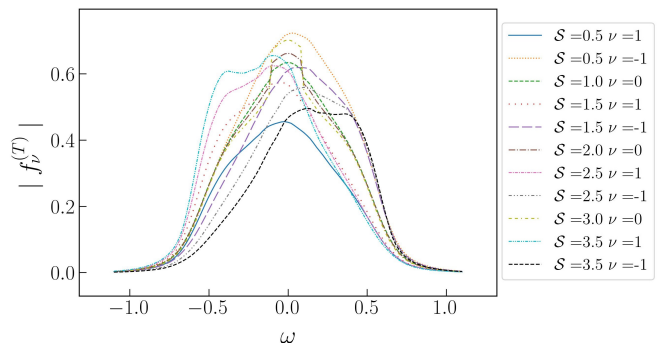


FIG. 6: Plots of $f_\nu^{(T)}(\mathcal{E}, \mathcal{S}, \omega)$ for the $T_0^{(1)}$ operator and $\mathcal{E} = 0$. We display plots for various values of \mathcal{S} and ν .

that $f_\nu^{(T)}(\mathcal{E}, \mathcal{S}, \omega)$ are smooth in ω in the thermodynamic limit.

We describe one method of calculating $f_\nu^{(T)}$ functions. First, we plot the off-block-diagonal reduced matrix elements as a three-dimensional (3D) scatter plot (Fig. 7). The reduced matrix elements lie on the z -axis, and energy values E_α and $E_{\alpha'}$ lie on the x and y axes, respectively. An example of this plot for 10 qubits and a $T_0^{(1)}$ operator is shown in Fig. 7. We then create a two-dimensional (2D) surface from the 3D scatterplot by averaging the reduced-matrix-element values in a small energy window to a single value. The energy windows have a width of 0.1 in E_α and $E_{\alpha'}$ across the entire range of E_α and $E_{\alpha'}$. Figure 8 displays an example of the 2D surface that Fig. 7 yields. From this 2D surface, we interpolate the reduced matrix element values along the $E_\alpha = E_{\alpha'}$ axis to obtain a 1D plot. The 1D plot displays the reduced matrix elements versus $\omega = E_\alpha - E_{\alpha'}$ and this yields $f_\nu^{(T)}(\mathcal{E}, \mathcal{S}, \omega)$ for a given \mathcal{E} and \mathcal{S} . Figures 7 - 9 show each step in the process of calculating $f_\nu^{(T)}(\mathcal{E}, \mathcal{S}, \omega)$. We

use 10 qubits for these plots because we were unable to use this method for larger system sizes, which required more computational resources than readily available.

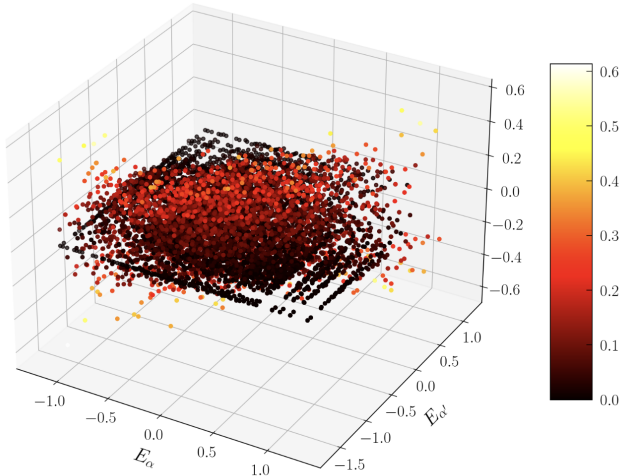


FIG. 7: Off-block-diagonal reduced matrix elements $\langle \alpha | T_0^{(1)} | \alpha \rangle$ in the $(s_\alpha = 2, s_{\alpha'} = 1)$ subspace for a system of 10 qubits.

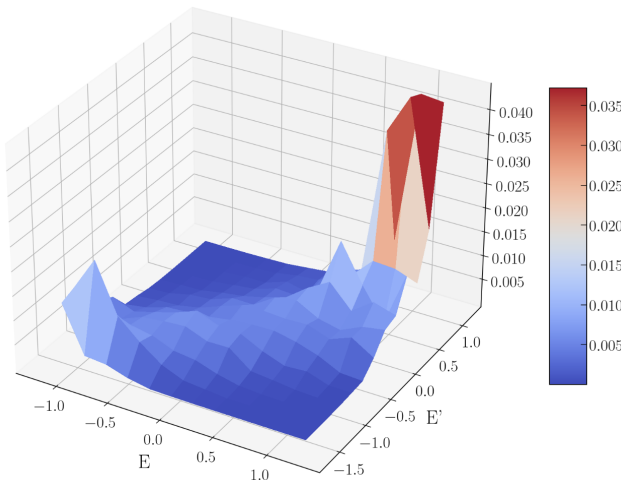


FIG. 8: Two-dimensional surface from averaging off-block-diagonal elements shown in Fig. 7 within E_α and $E_{\alpha'}$ windows of width 0.1. The off-block-diagonal reduced matrix elements are $\langle \alpha | T_0^{(1)} | \alpha \rangle$ in the $(s_\alpha = 2, s_{\alpha'} = 1)$ subspace for a system of 10 qubits.

IV B. Support for the FDT and KMS condition

We report on the ongoing calculations determining how well a system that obeys the NAETH also satisfies the KMS condition. Recall that for two eigenenergies E_α and $E_{\alpha'}$, the average energy is $\mathcal{E} = (E_\alpha + E_{\alpha'})/2$, the average spin quantum number is $\mathcal{S} = (s_\alpha + s_{\alpha'})/2$, and

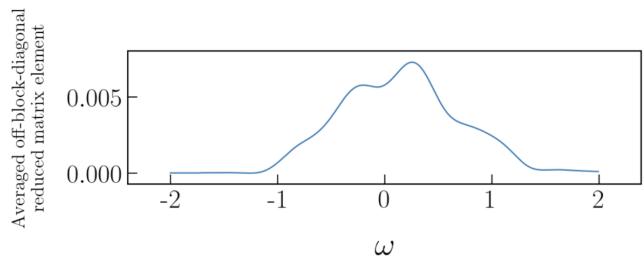


FIG. 9: $f_\nu^{(T)}(\mathcal{E} = 0, \mathcal{S} = 1.5, \omega)$ interpolated from the coarse-grained surface of off-block-diagonal elements for 10 qubits (Fig. 8).

the spin quantum number difference is $\nu = s_\alpha - s_{\alpha'}$. The NAETH's off-block-diagonal term contains the factor $f_\nu^{(T)}(\mathcal{E}, \mathcal{S}, \omega)$ (see Eq. 7). These $f_\nu^{(T)}$ functions appear in the time correlation function equation derived from the ETH [21]. When we use similar methods to derive a time correlation function from the NAETH, we have a similar dependence on $f_\nu^{(T)}$ functions. Our analytical and numerical work on determining whether a system following the NAETH satisfies the KMS condition is ongoing.

Two calculations we have completed toward this goal are computing $\mathcal{F}_\nu(E, \mathcal{S}, \omega)$ functions and the derivative $\frac{\partial \mathcal{F}_\nu}{\partial \mathcal{S}}$ of \mathcal{F} with respect to \mathcal{S} . Both of these terms are found in the finite-system-size correction term given by Eq. 11. For the first calculation, $\mathcal{F}_\nu(E, \mathcal{S}, \omega) := f_{-\nu}(E, \mathcal{S}, -\omega)f_\nu(E, \mathcal{S}, \omega)$. We reuse the f functions from Sec. IV A to plot \mathcal{F}_ν against ω . Figures 10 and 11 display \mathcal{F}_ν versus ω for 18 qubits and spherical tensor operators $T_0^{(1)}$ and $T_0^{(2)}$, respectively. The second calculation requires approximating the derivative $\frac{\partial \mathcal{F}_\nu}{\partial \mathcal{S}}$ using the discrete s_α we have. Figure 12 shows the plots of $\frac{\partial \mathcal{F}_\nu}{\partial \mathcal{S}}$ around the value of $\mathcal{S} = 2.0$. With \mathcal{F}_ν and $\frac{\partial \mathcal{F}_\nu}{\partial \mathcal{S}}$ of \mathcal{F} , our next step is to numerically calculate the entire finite-system-size correction term. We leave this as future work.

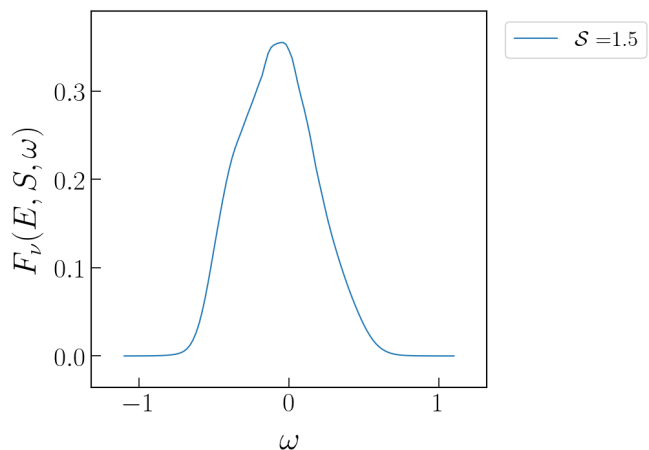


FIG. 10: Plot of $\mathcal{F}_\nu(\mathcal{E} = 0, \mathcal{S} = 1.5, \omega)$ for a system of 18 qubits and the $T_0^{(1)}$ operator.

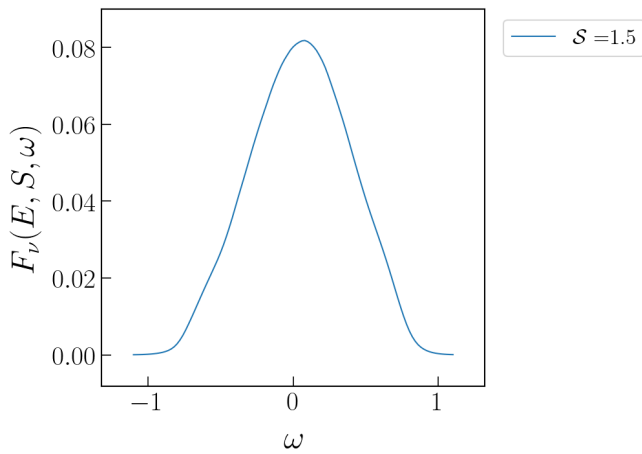


FIG. 11: Plot of $\mathcal{F}_\nu(\mathcal{E}=0, S=1.5, \omega)$ for a system of 18 qubits and the $T_0^{(2)}$ operator.

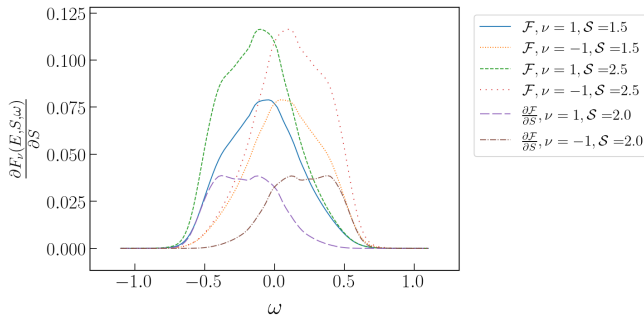


FIG. 12: Plot of $\frac{\partial \mathcal{F}_\nu(\mathcal{E}, S, \omega)}{\partial S}$ versus ω for $\mathcal{E}=0$, $S=2.0$, and $\nu=\pm 1$. The $\frac{\partial \mathcal{F}_\nu}{\partial S}$ s are calculated from the \mathcal{F}_ν functions. The $\frac{\partial \mathcal{F}_\nu}{\partial S}$ s will be used in the future to check the finite-system-size correction term.

V. CONCLUSIONS

Non-Abelian thermodynamics is an active area of research with new fundamental physics results and practical applications. The ETH is a key finding in many-body physics describing how a closed quantum many-body system thermalizes internally. When the system conserves quantities that fail to commute with each other, i.e., the system has a non-Abelian symmetry, the ETH no longer holds. The NAETH remedies the conflict between the ETH and non-Abelian symmetries. We have provided numerical support for the NAETH, confirming four of its qualitative predictions. The block-diagonal and off-block-diagonal reduced matrix elements both follow normal distributions, as we expect. We find evidence that the functions in the NAETH's off-block-diagonal term are smooth in some variables in the thermodynamic limit. We compute and plot functions that appear in the finite-size-correction term for correlation functions

derived from the NAETH. Our results invite further numerical and experimental testing of the NAETH.

We will extend our NAETH numerics to the FDT and KMS condition. Correlation functions in the FDT can be derived in the framework of the ETH. These correlation functions satisfy the KMS condition. For a system with a non-Abelian symmetry, we will derive similar correlation functions and check if they satisfy the KMS condition. Our analytics and numerics use finite system sizes, which yields a finite-system-size correction term to the correlation functions. In the future, we want to compare how the finite-system-size correction term for correlation functions from the ETH and NAETH scale. We aim to establish the first analytical and numerical support for a FDT governing a closed quantum many-body system with a non-Abelian symmetry.

VI. ACKNOWLEDGEMENTS

I am grateful for Dr. Nicole Yunger Halpern's and Dr. Aleksander Lasek's guidance and mentorship as I begin my research career. I'd like to thank JaeDong Noh for the rich collaboration on our projects. This work was supported by the National Science Foundation (QLCI grant OMA-2120757 and NSF award DMS-2231533) and Innovation, Science, and Economic Development (ISED) Canada.

REFERENCES

- [1] P. P. Potts, Quantum thermodynamics (2024), arXiv:2406.19206 [quant-ph].
- [2] S. Deffner and S. Campbell, *Quantum Thermodynamics*, 2053-2571 (Morgan Claypool Publishers, 2019).
- [3] S. Majidy, W. F. Braasch Jr., A. Lasek, T. Upadhyaya, A. Kalev, and N. Yunger Halpern, Noncommuting conserved charges in quantum thermodynamics and beyond, *Nature Reviews Physics* **5**, 689 (2023).
- [4] N. Y. Halpern, Beyond heat baths ii: framework for generalized thermodynamic resource theories, *Journal of Physics A: Mathematical and Theoretical* **51**, 094001 (2018).
- [5] Y. Guryanova, S. Popescu, A. J. Short, R. Silva, and P. Skrzypczyk, Thermodynamics of quantum systems with multiple conserved quantities, *Nature Communications* **7**, 1 (2016).
- [6] M. Lostaglio, *Thermodynamics at the quantum scale: Generalized Landauer principle*, Master's thesis, Imperial College London (2014).
- [7] T. Upadhyaya, W. F. Braasch, G. T. Landi, and N. Yunger Halpern, Non-abelian transport distinguishes three usually equivalent notions of entropy production, *PRX Quantum* **5**, 030355 (2024).
- [8] G. Manzano, J. M. Parrondo, and G. T. Landi, Non-abelian quantum transport and thermosqueezing effects, *PRX Quantum* **3**, 010304 (2022).
- [9] A. C. Potter and R. Vasseur, Symmetry constraints on many-body localization, *Phys. Rev. B* **94**, 224206 (2016).

- [10] I. V. Protopopov, W. W. Ho, and D. A. Abanin, Effect of $su(2)$ symmetry on many-body localization and thermalization, *Phys. Rev. B* **96**, 041122 (2017).
- [11] J. M. Deutsch, Quantum statistical mechanics in a closed system, *Phys. Rev. A* **43**, 2046 (1991).
- [12] M. Srednicki, Chaos and quantum thermalization, *Phys. Rev. E* **50**, 888 (1994).
- [13] M. Rigol, V. Dunjko, and M. Olshanii, Thermalization and its mechanism for generic isolated quantum systems, *Nature* **452**, 854 (2008).
- [14] A. P. Luca D'Alessio, Yariv Kafri and M. Rigol, From quantum chaos and eigenstate thermalization to statistical mechanics and thermodynamics, *Advances in Physics* **65**, 239 (2016), <https://doi.org/10.1080/00018732.2016.1198134>.
- [15] C. Gogolin and J. Eisert, Equilibration, thermalisation, and the emergence of statistical mechanics in closed quantum systems, *Reports on Progress in Physics* **79**, 056001 (2016).
- [16] C. Murthy, A. Babakhani, F. Iniguez, M. Srednicki, and N. Yunger Halpern, Non-abelian eigenstate thermalization hypothesis, *Phys. Rev. Lett.* **130**, 140402 (2023).
- [17] J. D. Noh, Eigenstate thermalization hypothesis in two-dimensional xxz model with or without $su(2)$ symmetry, *Phys. Rev. E* **107**, 014130 (2023).
- [18] A. Lasek, J. D. Noh, J. LeSchack, and N. Y. Halpern, Numerical evidence for the non-abelian eigenstate thermalization hypothesis (2024), arXiv:2412.07838 [quant-ph].
- [19] P. Coleman, Fluctuation–dissipation theorem and linear response theory, in *Introduction to Many-Body Physics* (Cambridge University Press, 2015) p. 292–331.
- [20] R. Kubo, The fluctuation-dissipation theorem, *Reports on Progress in Physics* **29**, 255 (1966).
- [21] J. D. Noh, T. Sagawa, and J. Yeo, Numerical verification of the fluctuation-dissipation theorem for isolated quantum systems, *Phys. Rev. Lett.* **125**, 050603 (2020).
- [22] J. D. Noh, A. Lasek, J. LeSchack, and N. Yunger Halpern, (in prep).
- [23] R. Shankar, *Principles of Quantum Mechanics*, 2nd ed. (Springer, New York, NY, 2008).
- [24] Y. Y. Atas, E. Bogomolny, O. Giraud, and G. Roux, Distribution of the ratio of consecutive level spacings in random matrix ensembles, *Phys. Rev. Lett.* **110**, 084101 (2013).